Analyst

PAPER

View Article Online
View Journal | View Issue

Cite this: *Analyst*, 2015, **140**, 5929

Identification of accelerants, fuels and post-combustion residues using a colorimetric sensor array†

Zheng Li, Minseok Jang, Jon R. Askim and Kenneth S. Suslick*

Received 24th April 2015,
Accepted 15th July 2015

DOI: 10.1039/c5an00806a

www.rsc.org/analyst

A linear (1 × 36) colorimetric sensor array has been integrated with a pre-oxidation technique for detection and identification of a variety of fuels and post-combustion residues. The pre-oxidation method permits the conversion of fuel vapor into more detectable species and therefore greatly enhances the sensitivity of the sensor array. The pre-oxidation technique used a packed tube of chromic acid on an oxide support and was optimized in terms of the support and concentration. Excellent batch to batch reproducibility was observed for preparation and use of the disposable pre-oxidation tubes. Twenty automotive fuels including gasolines and diesel from five gasoline retailers were individually identifiable with no confusions or misclassifications in quintuplicate trials. Limits of detection were at sub-ppm concentrations for gasoline and diesel fuels. In addition, burning tests were performed on commonly used fire accelerants, and clear differentiation was achieved among both the fuels themselves and their volatile residues after burning.

Introduction

Fire incidents, both accidental and malicious, have become a pressing issue in modern life due to their threat to human life, property, and environmental safety. According to reports from the US Fire Administration, over 1.5 million fires occurred throughout the US in 2013 which caused over 3000 deaths, 17 000 injuries and $10 billion in property damage.[1] Automotive fuels and other petroleum products such as gasoline, diesel, and kerosene are commonly employed as accelerants in case of arson; rapid discrimination among accelerants is therefore particularly important for fire scene investigation.[2–7] Additionally, the need for simple field-deployable quality control of automotive fuels has drawn great attention because of the negative effects caused by the adulteration of gasoline or diesel (*e.g.*, engine damage and air pollution),[8,9] and the fuel oil industry has suffered from fraudulent mixing of low-priced reagents with higher-priced fuels.[10]

Currently, the detection of fire accelerants is generally determined by standard analytical methods including electrochemistry,[9,11] fluorescence,[12] Fourier transform infrared spectroscopy (FTIR),[13–15] Raman spectroscopy,[2,16,17] GC[13,18] or GC–MS,[19–21] most of which demand non-portable and expensive instrumentation. Canine teams offer a more easily fielded approach for detecting accelerants in fire debris, though results are less reliable than traditional analytical methods as they are subject to human interpretation of a dog's responses; in addition, training dogs requires substantial time and effort.[22] Some commercialized hydrocarbon gas analyzers can detect and quantify flammable accelerants by vapor sampling, but are unable to identify specifically which accelerant is present.[23,24] Numerous other detection methods still suffer from high cost, low sensitivity, lack of reproducibility, interference from humidity, or changeable responses due to sensor aging.[25,26] For these reasons, the development a high-performance portable sensor for the on-site analysis of fire accelerants or quality control of fuels remains an important goal.

In the past decade, the use of disposable colorimetric sensor arrays (CSAs) has been developed for a variety of vapor analyses.[27–29] CSAs use strong chemical interactions between the analytes and a diverse set of cross-responsive chemoresponsive dyes; digital imaging of the arrays permits identification of a composite pattern of response as the "fingerprint" for a given odorant.[27–33] These arrays take advantage of plasticized films or organically modified siloxanes (ormosils) as matrices for colorants whose color changes are affected by polarity/dipolarity, Brønsted and Lewis acid–base interactions, redox reactions, and π–π interactions.[27–29]

Although colorimetric sensor arrays perform well for a variety of gases and volatile liquids,[34–36] they have not shown high sensitivity to less-reactive analytes, such as aliphatic and

Department of Chemistry, University of Illinois at Urbana-Champaign, 600 South Mathews Avenue, Urbana, Illinois 61801, USA. E-mail: ksuslick@illinois.edu

†Electronic supplementary information (ESI) available. See DOI: 10.1039/c5an00806a

aromatic hydrocarbons or halocarbons.[30,37] A typical gasoline consists of 30–50% alkanes, 5–10% alkenes and 20–40% aromatics and therefore does not respond to a sensor array designed for strong chemical interactions. We have previously shown that substantial improvements in the detection, identification, and quantitation of less-reactive volatiles can be made by employing a pre-treatment technique in which the analyte gas stream is subjected to partial oxidation and thus converted into more easily detected oxidation products (*e.g.*, aldehydes and carboxylic acids).[37] We demonstrate here that this technique can be extended for the identification of complex fuel mixtures and have examined discrimination among a large number of commercial fuels, differentiating among both the fuels themselves and their volatile residues after burning.

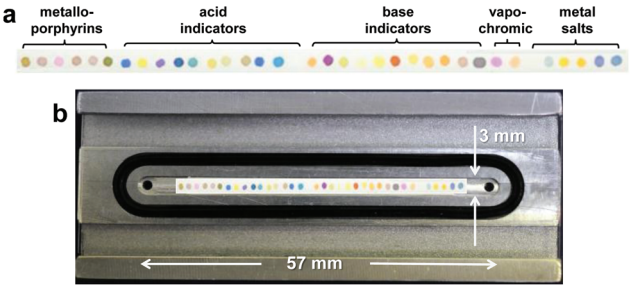

Fig. 1 Photographs of the colorimetric sensor array used for fuel detection. (a) Linear 36-spot colorimetric sensor array containing metalloporphyrins, acid- or base-treated pH indicators, solvatochromic/vapochromic and metal-containing dyes; (b) colorimetric sensor array mounted in an aluminum holder with an o-ring placed in a groove and a glass slide cover in place; this provides a nearly ideal flow path for the analyte stream with a flow volume of ~85 μL.

Experimental

Chemicals and materials

For the gasolines used in these experiments, we provide their brand name and average octane number (ON = $(R + M)/2$, where R is the research octane number and M is the motor octane number).[38] Three different grades of gasoline (*i.e.*, regular, ON87; plus, ON89; and premium, ON93) and diesel fuel were purchased from five local gasoline distributors (*i.e.*, Mobil, Marathon, Shell, BP and Schnucks). Ethanol, i-propanol, kerosene, mineral oil, aluminum oxides (Brockmann I, Sigma-Aldrich), silica gels (Davisil, Sigma-Aldrich) and all other reagents were of analytical-reagent grade and used without further purification unless otherwise specified. Lubricant (WD-40 type 110071), vegetable oil (Great Value) and nylon carpet (Guardian, platinum series) were purchased from a local supermarket.

Formulations, preparation and sensor array printing

Sol–gel pigments were prepared as previously described.[39,40] Sol–gel formulations were obtained *via* the acid catalyzed hydrolysis of silane precursors (*e.g.*, mixtures of tetraethoxysilane (TEOS), methyltriethoxysilane (MTEOS), octyltriethoxysilane (octyl-TEOS)). The resulting ormosil formulations after hydrolysis were added to the 36 selected dyes (ESI, Table S1†) and then loaded into a 36-hole Teflon inkwell. Sensor arrays were printed on a robotic microarray printer (Arraylt Co., Mountain View, CA) by dipping slotted pins into the inkwell and delivering the formulation (~100 nL) to a polyvinylidene difluoride (PVDF) membrane (Fig. 1a). Once printed, the arrays were stored in a N_2-filled glove bag for three days. Each array was then cut into strips and mounted in a custom made aluminum flow cell, with channel dimensions of 3.0 × 0.5 × 57 mm (Fig. 1b). A Viton o-ring is placed in a groove around the channel and a standard glass microscope slide is clamped to create a leak-free seal that permits a gas analyte stream to flow over the sensor array.

Preparation of pre-oxidation tube

The oxidizing agent (chromic acid loaded on an inert oxide support) was made as previously reported[37] by mixing alumina or silica (2.5 g), $Na_2Cr_2O_7$ (1.0 g), 98% H_2SO_4 (1.0 mL), and H_2O (10.0 mL). Water was removed under vacuum at 60 °C for 0.5 h. The resulting gel was further dried by flowing dry nitrogen for 4 h. 40 mg of oxidizing agent were packed into the middle of a Teflon tube (3.2 mm inner diameter), sealed with glass wool on both ends (ESI, Fig. S1†).

Analyte vapor generation

Analyte flow streams were produced by bubbling dry nitrogen through the liquid fuels (ESI, Fig. S2A†), or by flushing dry nitrogen over a carpet sample (2.5 × 2.5 cm nylon carpet samples loaded with 1 mL of accelerant with or without burning for 1 min, as shown in ESI, Fig. S2B†). The resulting vapor streams were then mixed with a diluting stream of dry and wet nitrogen to attain the desired concentrations at 50% relative humidity (RH) by using MKS digital mass flow controllers (MFCs). For all the experiments performed in this study, the flow rate was 500 sccm. The response of the sensor array essentially reaches equilibrium during the first minute and is not dependent (after equilibration) on flow rate or dose. All data was compared after equilibration after 1 min exposure to the analyte flow.

Digital imaging and data analysis

For all sensing experiments, sensor arrays were imaged on a flatbed scanner (Epson Perfection V600). The array was equilibrated with 50% RH nitrogen for 1 min at a flow rate of 500 sccm to capture the before-exposure image, and after-exposure image was acquired after 1 min exposure to the fuel or post-combustion vapor at 500 sccm. Difference maps were obtained by subtracting the red, green, and blue (RGB) values of before-exposure images from those of after-exposure images; each sensor spot was ~100 pixels, the values of which were averaged. Digitization of the color differences was performed using a customized software package, SpotFinder 1.0.6 (iSense LLC., Mountain View, CA). Chemometric analysis was carried out on 108-dimensional color difference vectors

(36 sets of ΔR, ΔG and ΔB values) using Multi-Variate Statistical Package™ (MVSP v.3.1, Kovach Computing); minimum variance (*i.e.*, "Ward's Method") was used for hierarchical cluster analysis (HCA) in all cases. The full digital database of sensor array responses is provided in the ESI (Tables S2, S3 and S4†).

Results and discussion

The chemical basis for discrimination among fuels is of course due to differences in their chemical composition. For gasolines and other complex fuel mixtures, there are three sources of such differences: (1) there are gross distinctions in composition between gasoline and diesel fuels (gasolines contain hydrocarbons that are generally lower molecular weight and more volatile); (2) composition depends on octane rating values (a relative measure of anti-knocking properties), which are sensitive to the concentrations of aromatic hydrocarbons or alcohols; and (3) each brand of gasoline has specific additives to the base gasoline that are brand specific and treated as trade secrets.

Optimization of pre-oxidation method

Substantial improvements in the detection, identification, and quantitation of less-reactive volatiles by colorimetric sensor arrays have been made by employing a pre-oxidation treatment in which the analyte gas stream is subjected to partial oxidation that creates more easily detected oxidation products (*e.g.*, aldehydes and carboxylic acids).[37] For the application to fuels, the choice of oxidizing reagent type was optimized by examining the performance of chromic acid loaded on nine separate supporting materials (alumina or silica gel) with different surface areas, ranging from 40 to 250 $m^2\ g^{-1}$ for alumina and from 300 to 675 $m^2\ g^{-1}$ for silica. Exposure to Marathon Regular (ON87) gasoline at 10% of its saturated vapor pressure for 1 min was used as a standardized evaluation of sensor array response for all optimization experiments. Surface area in this case is a double-edged sword: materials with high surface area tend to absorb oxidation products while materials with low surface area do not offer enough retention time or active surface area for analytes to react with the pre-oxidation media (Fig. 2 and S3A†). The optimal support material was found to be alumina powder with ~100 $m^2\ g^{-1}$ surface area. The dependence of array response on the amount of the oxidation reagent was investigated; as shown in Fig. S3B,† array responses are optimized at ~40 mg of supported oxidant. The optimal response time was illustrated in the response curves of various pre-oxidation reagents over 5 min of exposure (Fig. S3C†); array responses fully equilibrated within the first min. For studies to demonstrate differentiation among fuels or post-oxidation residues, these optimized conditions for the pre-oxidation method were fixed to a load of 40 mg of 30 wt% chromic acid on alumina (surface area ~100 $m^2\ g^{-1}$), 500 sccm flow rate, and 1 min exposure time.

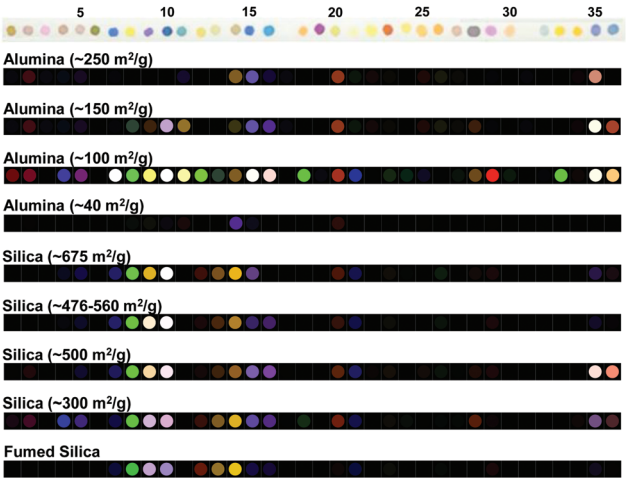

Fig. 2 Color difference maps for nine kinds of pre-oxidation reagents with chromic acid on different oxide supports after 1 min exposure to Mobil 87 gasoline at 10% of saturation. For display purposes, the color range has been expanded from 5 bits (4–35) to 8 bits (0–255).

Discrimination of automotive fuels

In prior studies using colorimetric sensor arrays to identify and quantify various volatile organic chemicals (VOCs) and toxic industrial chemicals (TICs), the range of concentrations that are important are well defined by the permissible exposure limits (PELs) and immediately dangerous to life or health (IDLH) concentrations,[28,37,39,40] In contrast, there are no explicit standards for essential detection concentrations of accelerants; for our studies here, two concentrations were arbitrarily chosen: 10% of the saturated vapor pressure as an upper concentration level and 1% of saturation (*e.g.*, ~7 ppm for diesel at 20 °C) as lower level.

In the absence of pre-oxidation, the colorimetric sensor array is not particularly sensitive to fuels or hydrocarbons.[37] We are able to gain significant response, however, to the partial oxidation products produced from fuels using our pre-oxidation technique: representative difference maps of 20 automotive fuels from 5 gas distributors (Mobil, Marathon, Shell, BP and Schnucks) at 10% of their saturated vapor pressure after 1 min exposure are shown in Fig. 3. The partial oxidation products (*e.g.*, aldehydes and carboxylic acids) interact with sensor spots containing acid-treated pH indicators (*i.e.*, spots 7–16) and metal–dye complexes (*i.e.*, spots 35 and 36). There are clearly strong similarities among all of the fuels color difference maps presented in Fig. 3. A more quantitative analysis of the color differences, however, requires a classification algorithm that makes use of the full dimensionality of the data. To that end, a simple and model-free method, hierarchical cluster analysis (HCA),[41–43] was used for a quantitative analysis of the database of array responses.

HCA generates a dendrogram based on the grouping of array response data in the 108-dimensional vector space (*i.e.*, 3 × 36 color difference changes in red, green and blue (RGB) values from the 36 chemically responsive colorants that make

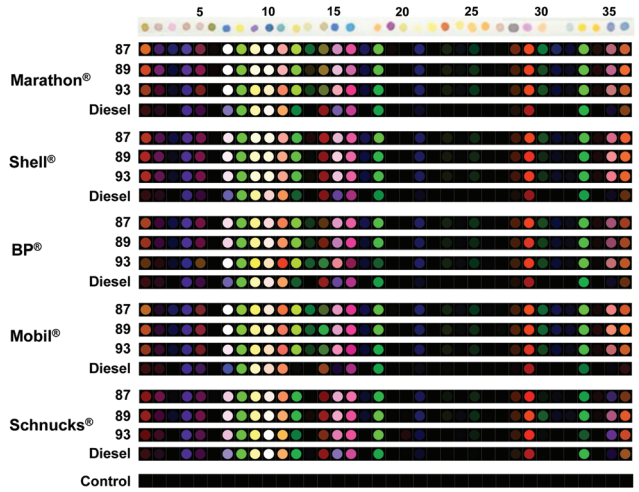

Fig. 3 Representative color difference maps showing quintuplicate analyses of 20 automotive fuels after pre-oxidation (octane number 87, ON89, ON93 gasolines and diesel from 5 commercial distributor brands) and a control after 1 min exposure at 10% of saturation. For display purposes, the color range has been expanded from 5 bits (4–35) to 8 bits (0–255).

up the sensor array). The HCA dendrogram (Fig. 4) shows excellent clustering into fuel types. There is a clear subdivision among the fuel analytes into gasoline *versus* diesel samples; this is due in part to the difference in their vapor pressures. Surprisingly, detailed clustering shows clear separation based on individual gasoline octane numbers and brands. Clustering by brand first and octane number second was clearly observed for Shell, BP and Schnucks brands, while Marathon ON93 clustered more closely to Mobil ON93 gasoline samples than other Marathon gasoline samples. Within the individual fuel types (brand and ON), among the quintuplicate trials of all 20 fuels at 10% of saturation and a blank control, there were no misclusterings observed in 105 cases.

Similar studies were done at 1% of saturation for the same fuels in order to probe the ability of the colorimetric sensor array to monitor low levels of vapors from automotive fuels. As with the higher-concentration samples, an exposure time of 1 min was sufficient to equilibrate the array response (ESI, Fig. S4†). The color difference maps are similar among the fuels at 1% of saturation, but again with subtle differences (ESI, Fig. S5†). The HCA dendrogram for the response of automotive fuels at 1% of saturation are shown in Fig. 5; again accurate discrimination among all 20 analytes and the nitrogen control is observed with no confusions or misclusterings out of 105 cases. Just as with the data collected at 10% of saturation, differentiation by brand and ON is seen for clustering of data at 1% of saturation.

Limit of detection (LOD) and limit of recognition (LOR)

We estimate the LOD for two fuel samples (Mobil ON87 and Mobil diesel) by extrapolating from the observed array responses at a series of five concentrations, as shown in ESI, Fig. S6.† LOD is defined as the concentration of the analyte needed to obtain three times the S/N *vs.* background for the largest signal among the 108 color changes. The detection limits are estimated to be 0.7 ppm for gasoline (*i.e.*, 0.003% of saturated vapor pressure) and 0.4 ppm for diesel (*i.e.*, 0.06% of saturated vapor pressure) based on their one minute response (where ppm refers to the total hydrocarbon gas phase concentration by volume).

Limits of recognition are, by definition, dependent upon the choice of analytes. The perfect clustering observed in the HCA dendrogram for 20 separate automotive fuels at 1% of

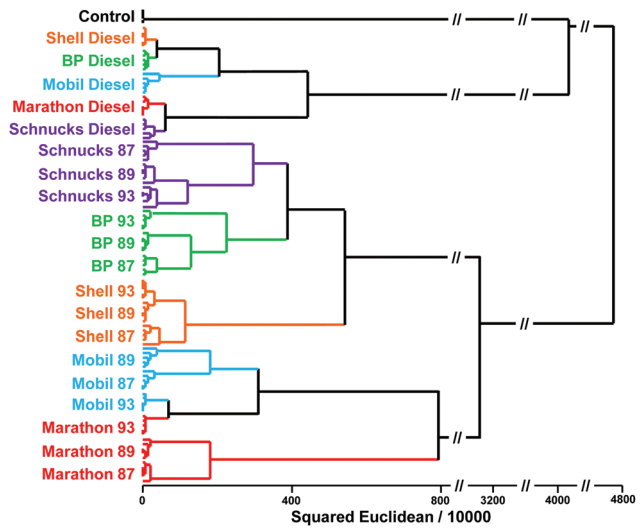

Fig. 4 Hierarchical cluster analysis (HCA) for 20 separate automotive fuels and one control. Each analyte name represents quintuplicate trials after 1 min exposure at 10% of saturated vapor pressure. No misclassifications or confusions were observed out of 105 total trials.

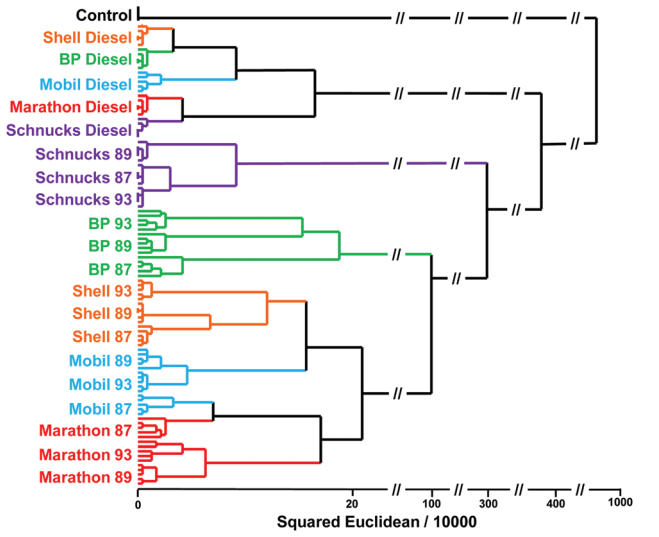

Fig. 5 Hierarchical cluster analysis (HCA) for 20 separate automotive fuels and one control. Each analyte name represents quintuplicate trials after 1 min exposure at 1% of saturated vapor pressure. No misclassifications or confusions were observed out of 105 total trials.

their saturated vapor pressure and one control, as shown in Fig. 5, establishes that our limits of recognition, for these analytes, are well below those concentrations (*e.g.*, roughly 250 ppm for gasolines and 7 ppm for diesel).

Detection of pre- or post-combustion residues

In an attempt to test accelerants after a simulated fire scenario, the colorimetric sensor array was used to detect and differentiate ignitable residues prior to or after combustion. To that end, 1 mL of each fire accelerant was dropped on a piece of nylon carpet (2.5 × 2.5 cm) and then ignited using a propane torch and allowed to burn for 1 min. After burning, carpet samples were allowed to cool down for 1 min and then transferred into a gas flow chamber for array analysis. 1 min cool-down was sufficient to bring the carpet sample to ambient temperature. Unburned ignitable residues were tested for comparison, and carpet samples without added accelerant (both burned and unburned) were used as controls. The same pre-oxidation technique described above was used in these studies.

Color difference maps of nine sets of burned or unburned residues plus two controls are shown in Fig. 6. Compared to the difference maps of fuels, the patterns shown for burned or unburned residues show a much broader range of response, which reflects the broader range of analytes present. The HCA dendrogram shown in Fig. 7 demonstrates excellent discrimination among all eighteen analytes and two controls. All twenty groups of analytes and controls were separated without confusions or misclusterings among 100 individual trials. There are two clearly distinct clusters: burned *versus* unburned samples with the exception of the four most weakly-responding analytes (burned and unburned vegetable oil and carpet).

Accelerants after burning generally show weaker responses than the unburned ones, likely due both to analyte evaporation

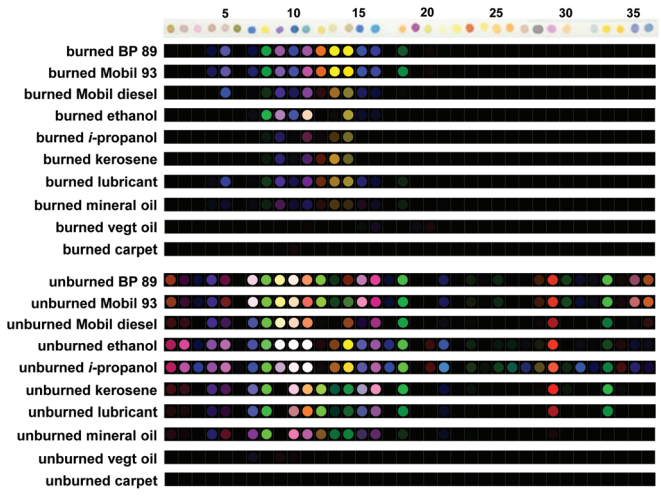

Fig. 6 Representative color difference maps showing quintuplicate runs of common fire accelerants and two controls after 1 min exposure at 10% of saturation using alumina pre-oxidation. For display purposes, the color range has been expanded from 5 bits (4–35) to 8 bits (0–255).

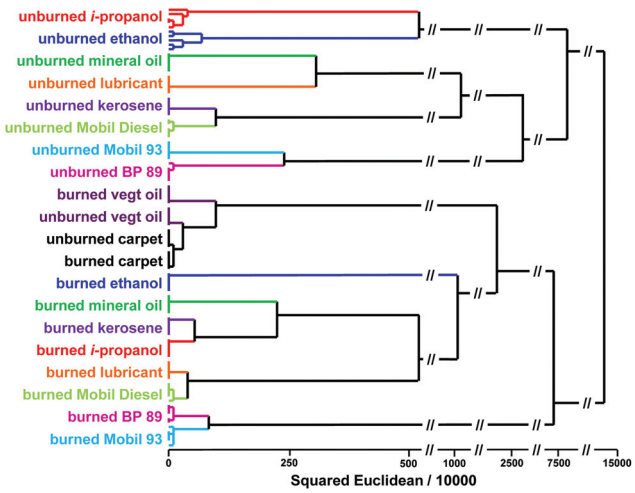

Fig. 7 Hierarchical cluster analysis (HCA) of unburned and burned accelerants from quintuplicate trials with 1 min exposure at 10% of saturation. Two separate clusters of burned and unburned residues were clearly observed, except for the most weakly-responding analytes (vegetable oil and controls).

and to the formation of gaseous combustion products (*i.e.*, CO_2 or CO) to which the sensor array is less responsive. Carpet samples burned in the absence of accelerates produce only very weak responses from the sensor array (Fig. 6). The somewhat stronger responses observed from burned accelerant samples are therefore attributable to the trace amounts of unburned volatiles or other byproducts from incomplete combustion of the accelerants.

Principal component analysis (PCA)

Principal component analysis (PCA)[41–44] was employed to provide an estimation of the dimensionality of the data acquired with the colorimetric sensor array, which is itself a measure of the dimensionality of the chemical reactivity space probed by the sensor array. PCA is an unsupervised and model-free statistical approach that generates a set of orthogonal eigenvectors (*i.e.*, principal components) using a linear combination of array response vectors to maximize the amount of variance in the fewest possible principal components.

If we consider all data collected in these studies (305 trials in 61 classes, as represented in Fig. S4, 5, and 7†), PCA reveals that 10 dimensions are required to capture 95% of the total variance and 28 dimensions are needed to capture 99%, as shown in the scree plot given in Fig. 8. There are also three subsets of the library database that have been analyzed individually by PCA: fuels at 10% of saturation (Fig. 4), fuels at 1% of saturation (Fig. 5), and the burn *vs.* unburned study (Fig. 7). For fuels at 10% of saturation, PCA required 4 dimensions to capture 95% of total variance and 12 dimensions for 99% (ESI, Fig. S7A†); for fuels at 1% of saturation, PCA required 6 dimensions for 95% of total variance and 13 dimensions for 99% (ESI, Fig. S7B†); and for the burned/unburned data, 8 dimensions for 95% of variance and 15 dimensions for 99% (ESI,

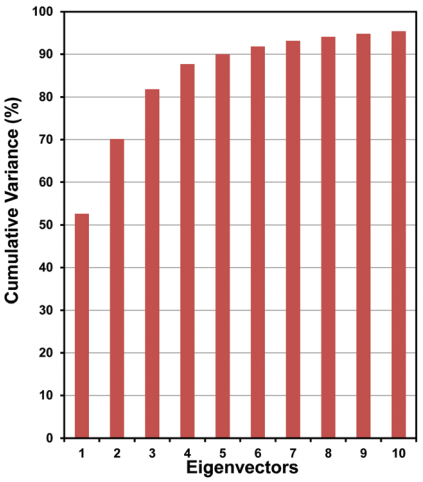

Fig. 8 Scree plot from a PCA for all 305 trials used in this study. 10 dimensions were required to capture 95% of the total variance.

Fig. S7C†). The high dimensionality shown in all of these studies reflects both the range of individual components produced during the pre-oxidation method and the broad range of chemical interactions probed by the chemically-responsive colorants that make up the sensor array.[27,30,34,36]

Classification by support vector machines (SVM)

We have used a common machine learning tool, SVM,[45] for a test of predictive classification of our datasets, making use of LIBSVM, an open-source SVM library.[46] Inherently, model-free clustering analyses, such as PCA or HCA, are not well suited for predictive (*i.e.*, classification) use. In contrast, SVM is a predictive approach that is designed to classify incoming data that does not belong to a pre-existing training database. SVM classifies an incoming test data point based on whether it lies above or below an optimized decision boundary for each possible choice between pairs of analyte classes. Classification accuracy can be estimated using cross-validation methods which split the database into training and evaluation subsets; the classifiers based on the training subset are tested with evaluation data subset. To test our SVM model, we have used a leave-one-out permutation method of cross-validation. As included in the digital database (ESI, Table S5†), in the permutated cross-validation of 305 trials in 61 classes, no errors in predictive classification are observed: *i.e.*, SVM predictions show an error rate of <0.3% in cross-validation classification tests. Similarly, if SVM cross-validation is applied to each of the three subsets of data, no errors are observed.

Reproducibility

To evaluate the reproducibility of our colorimetric sensor array, 3 new samples of previously tested BP gasolines (BP 87, 89 and 93) were purchased six months later and were tested in quintuplicate as new entries into the database at 1% of saturation; as a further test of reproducibility, the sensor arrays came from multiple printings in these studies. As shown in ESI, Fig. S8,† the two different sets of the three gasolines gave nearly identical array responses, and discrete clusters as a function of the octane numbers were still observed in the HCA for each kind of BP gasoline.

The reproducibility of the pre-oxidation method is also critical to our ability to differentiate among similar fuels. Given the inherent reactivity of chromic acid, issues of reproducible preparation of the oxidation tubes might have been a potential problem. To test this issue, we prepared three separate batches of chromic acid on alumina were prepared and tested each batch in quintuplicate with Mobil diesel fuel at 1% of saturation. As shown in ESI, Fig. S9,† excellent reproducibility of the oxidizing reagent is observed among the three batches, and in all cases, Mobil diesel is well differentiated from the other four brands of diesel fuel.

Conclusions

A disposable colorimetric sensor array has been developed in combination with pre-oxidation technique that shows substantial capability of detecting and identifying a variety of automotive fuels and commonly used fire accelerants. By testing the partial oxidation products produced by passing fuel vapor streams through an oxidant tube (chromic acid on alumina), the sensor array could distinguish among subtle differences in common fuels (type, octane ratings, and brand) at both high (10% of saturation) and low (1% of saturation) vapor concentration levels. Limits of detection are estimated to be 0.7 ppm for gasoline (*i.e.*, 0.003% of saturated vapor pressure) and 0.4 ppm for diesel (*i.e.*, 0.06% of saturated vapor pressure) based on their one minute response. Limits of recognition (which are analyte choice dependent) are well below 1% of saturated vapor pressure for the library of 20 separate automotive fuels and the control. Simulated burning tests also showed significant discrimination among other common fire accelerants such as kerosene, oils, and alcohols. Principal component analysis demonstrated high dimensionality in the data from the colorimetric sensor arrays with the pre-oxidation tube (10 dimensions to capture 90% of the total variance). As a consequence, hierarchical cluster analysis showed excellent discrimination among 61 classes of analytes, and support vector machine analysis showed no errors (<0.3% among 305 trials) in cross-validation classification tests. Finally, the colorimetric sensor array showed excellent reproducibility towards different purchases of the same fuel and different batches of the oxidizing reagent. This technology may find applications for quality control of fuel production and distribution as well as forensic investigation of fire scenes.

Acknowledgements

This work was supported by the U.S. NSF (CHE-1152232) and the U.S. Dept. of Defense (JIEDDO/TSWG CB3614). Financial support by CTTSO/JIEDDO does not constitute an express or

implied endorsement of the results or conclusions of the project by either CTTSO/JIEDDO or the U.S. Dept. of Defense.

Notes and references

1 U.S. Fire Administration, http://www.usfa.fema.gov/data/statistics accessed 04/10/2015.
2 K. M. Tan, I. Barman, N. C. Dingari, G. P. Singh, T. F. Chia and W. L. Tok, *Anal. Chem.*, 2012, **85**, 1846–1851.
3 P. M. L. Sandercock, *Forensic Sci. Int.*, 2008, **176**, 93–110.
4 S. Zhuiykov, *Sens. Actuators, A*, 2008, **141**, 89–96.
5 N. D. K. Petraco, M. Gil, P. A. Pizzola and T. A. Kubic, *J. Forensic Sci.*, 2008, **53**, 1092–1101.
6 T. A. Brettell, J. M. Butler and J. R. Almirall, *Anal. Chem.*, 2011, **83**, 4539–4556.
7 P. Vergeer, A. Bolck, L. J. C. Peschier, C. E. H. Berger and J. N. Hendrikse, *Sci. Justice*, 2014, **54**, 401–411.
8 T. Sobański, A. Szczurek, K. Nitsch, B. W. Licznerski and W. Radwan, *Sens. Actuators, B*, 2006, **116**, 207–212.
9 L. Bueno and T. R. L. C. Paixão, *Talanta*, 2011, **87**, 210–215.
10 S. Suwanprasop, T. Nhujak, S. Roengsumran and A. Petsom, *Ind. Eng. Chem. Res.*, 2004, **43**, 4973–4978.
11 N. K. L. Wiziack, A. Catini, M. Santonico, A. D'Amico, R. Paolesse, L. G. Paterno, F. J. Fonseca and C. Di Natale, *Sens. Actuators, B*, 2009, **140**, 508–513.
12 M. J. Aernecke and D. R. Walt, *J. Forensic Sci.*, 2010, **55**, 178–184.
13 E. Scorsone, A. M. Pisanelli and K. C. Persaud, *Sens. Actuators, B*, 2006, **116**, 55–61.
14 M. A. Al-Ghouti, Y. S. Al-Degs and M. Amer, *Talanta*, 2008, **76**, 1105–1112.
15 J. W. Diehl, J. W. Finkbeiner and F. P. DiSanzo, *Anal. Chem.*, 1995, **67**, 2015–2019.
16 M. Ahmadjian and C. W. Brown, *Anal. Chem.*, 1976, **48**, 1257–1259.
17 J. B. Cooper, K. L. Wise, J. Groves and W. T. Welch, *Anal. Chem.*, 1995, **67**, 4096–4100.
18 M. E. Sigman, M. R. Williams and R. G. Ivy, *Anal. Chem.*, 2007, **79**, 3462–3468.
19 Y. Lu and P. B. Harrington, *Anal. Chem.*, 2007, **79**, 6752–6759.
20 M. Monfreda and A. Gregori, *J. Forensic Sci.*, 2011, **56**, 372–380.
21 N. A. Sinkov, P. M. L. Sandercock and J. J. Harynuk, *Forensic Sci. Int.*, 2014, **235**, 24–31.
22 M. E. Kurz, S. Schultz, J. Griffith, K. Broadus, J. Sparks and G. Dabdoub, *J. Forensic Sci.*, 1996, **41**, 868–873.
23 M. D. Goldthorp and P. Lambert, *J. Hazard. Mater.*, 2001, **83**, 135–152.
24 K.-H. Kim and R. Pal, *Sens. Actuators, B*, 2008, **134**, 832–838.
25 F. Röck, N. Barsan and U. Weimar, *Chem. Rev.*, 2008, **108**, 705–725.
26 R. A. Potyrailo, C. Surman, N. Nagraj and A. Burns, *Chem. Rev.*, 2011, **111**, 7315–7354.
27 J. R. Askim, M. Mahmoudi and K. S. Suslick, *Chem. Soc. Rev.*, 2013, **42**, 8649–8682.
28 S. H. Lim, L. Feng, J. W. Kemling, C. J. Musto and K. S. Suslick, *Nat. Chem.*, 2009, **1**, 562–567.
29 K. S. Suslick, *MRS Bull.*, 2004, **29**, 720–725.
30 M. C. Janzen, J. B. Ponder, D. P. Bailey, C. K. Ingison and K. S. Suslick, *Anal. Chem.*, 2006, **78**, 3591–3600.
31 M. K. LaGasse, J. M. Rankin, J. R. Askim and K. S. Suslick, *Sens. Actuators, B*, 2014, **197**, 116–122.
32 N. A. Rakow and K. S. Suslick, *Nature*, 2000, **406**, 710–714.
33 J. W. Kemling, A. J. Qavi, R. C. Bailey and K. S. Suslick, *J. Phys. Chem. Lett.*, 2011, **2**, 2934–2944.
34 B. A. Suslick, L. Feng and K. S. Suslick, *Anal. Chem.*, 2010, **82**, 2067–2073.
35 C. Zhang and K. S. Suslick, *J. Agric. Food Chem.*, 2007, **55**, 237–242.
36 J. R. Carey, K. S. Suslick, K. I. Hulkower, J. A. Imlay, K. R. C. Imlay, C. K. Ingison, J. B. Ponder, A. Sen and A. E. Wittrig, *J. Am. Chem. Soc.*, 2011, **133**, 7571–7576.
37 H. Lin, M. Jang and K. S. Suslick, *J. Am. Chem. Soc.*, 2011, **133**, 16786–16789.
38 W. Dabelstein, A. Reglitzky, A. Schütze and K. Reders, Automotive fuels, in *Ullmann's Encyclopedia of Industrial Chemistry*, Wiley-VCH, Weinheim, 2012.
39 L. Feng, C. J. Musto, J. W. Kemling, S. H. Lim and K. S. Suslick, *Chem. Commun.*, 2010, **46**, 2037–2039.
40 L. Feng, C. J. Musto, J. W. Kemling, S. H. Lim, W. Zhong and K. S. Suslick, *Anal. Chem.*, 2010, **82**, 9433–9440.
41 J. F. Hair, B. Black, B. Babin, R. E. Anderson and R. L. Tatham, *Multivariate Data Analysis*, Prentice Hall, New York, 6th edn, 2005.
42 J. Janata, *Principles of Chemical Sensors*, Springer, New York, 2nd edn, 2009.
43 R. A. Johnson and D. W. Wichern, *Applied Multivariate Statistical Analysis*, Prentice Hall, New York, 6th edn, 2007.
44 S. Stewart, M. A. Ivy and E. V. Anslyn, *Chem. Soc. Rev.*, 2014, **43**, 70–84.
45 I. Steinwart and A. Christmann, *Support Vector Machines*, Springer, New York, 2008.
46 C.-C. Chang and C.-J. Lin, *ACM Trans. Intell. Syst. Technol.*, 2011, **2**, 1–27.